

# Chemical Vapor Detection Using a Capacitive Micromachined Ultrasonic Transducer

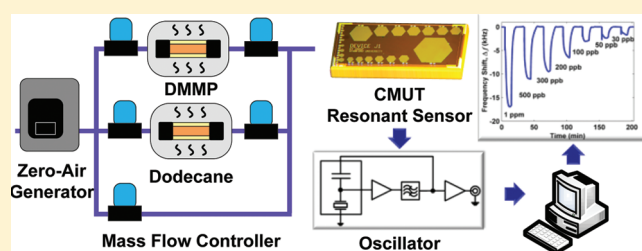
Hyunjoo J. Lee,<sup>\*,†</sup> Kwan Kyu Park,<sup>†</sup> Mario Kupnik,<sup>§</sup> Ö. Oralkan,<sup>†</sup> and Butrus T. Khuri-Yakub<sup>†</sup>

<sup>†</sup>Edward L. Ginzton Laboratory, Stanford University, Stanford, California 94305, United States

<sup>§</sup>Brandenburg University of Technology, 03046 Cottbus, Germany

**S** Supporting Information

**ABSTRACT:** Distributed sensing of gas-phase chemicals using highly sensitive and inexpensive sensors is of great interest for many defense and consumer applications. In this paper we present ppb-level detection of dimethyl methylphosphonate (DMMP), a common simulant for sarin gas, with a ppt-level resolution using an improved capacitive micromachined ultrasonic transducer (CMUT) as a resonant chemical sensor. The improved CMUT operates at a higher resonant frequency of 47.7 MHz and offers an improved mass sensitivity of 48.8 zg/Hz/ $\mu\text{m}^2$  by a factor of 2.7 compared to the previous CMUT sensors developed. A low-noise oscillator using the CMUT resonant sensor as the frequency-selective device was developed for real-time sensing, which exhibits an Allan deviation of 1.65 Hz ( $3\sigma$ ) in the presence of a gas flow; this translates into a mass resolution of 80.5 zg/ $\mu\text{m}^2$ . The CMUT resonant sensor is functionalized with a 50-nm thick DKAP polymer developed at Sandia National Laboratory for dimethyl methylphosphonate (DMMP) detection. To demonstrate ppb-level detection of the improved chemical sensor system, the sensor performance was tested at a certified lab (MIT Lincoln Laboratory), which is equipped with an experimental chemical setup that reliably and accurately delivers a wide range of low concentrations down to 10 ppb. We report a high volume sensitivity of  $34.5 \pm 0.79$  pptv/Hz to DMMP and a good selectivity of the polymer to DMMP with respect to dodecane and 1-octanol.



Miniaturized chemical sensors based on microelectromechanical systems (MEMS) offer competitive advantages over existing benchtop chemical analyzers, such as small size, low power consumption, low cost due to batch fabrication, and CMOS compatibility. The potential for system integration of these chemical sensors with on-chip CMOS circuitry expands the spectrum of use, including consumer, industrial, military, and homeland security applications. For example, one can envision a network of chemical sensors embedded in every smartphone that monitors air quality and tracks climate change by recording the  $\text{CO}_2$  levels and temperature. A portable chemical sensor that can detect a very small trace of chemical warfare agents is also critical for military and counterterrorism applications, such as protecting soldiers from improvised explosive devices on the modern battlefield.

Resonant sensors based on the mass-loading mechanism provide a number of advantages over the sensors that are based on other physical parameters such as capacitance,<sup>1</sup> resistance,<sup>2</sup> and deflection.<sup>3</sup> First, resonant sensors offer superior sensitivity and resolution because of the high noise immunity owing to high- $Q$  resonance. In addition, because the output range of resonant sensors is not limited by the supply voltage, the resonant sensors typically offer a wide dynamic range.<sup>4</sup> As a result, many MEMS resonant devices including cantilevers,<sup>5</sup> thin film bulk acoustic resonators (FBAR),<sup>6</sup> and surface acoustic wave (SAW) resonators<sup>7</sup> have been proposed as a platform for miniaturized chemical sensor systems. However, only a few systems achieve mass resolutions

below attogram ( $10^{-18}$  g) level and volume sensitivity to chemical warfare agents below parts-per-billion (ppb).

This paper introduces a miniaturized resonant chemical sensor system based on a capacitive micromachined ultrasonic transducer. The system demonstrates a significant improvement in the mass and volume sensitivity to dimethyl methylphosphonate (DMMP), a common simulant for sarin gas in air. Our results show that the CMUT is an excellent candidate as a miniaturized chemical sensor system because it offers several advantages over existing MEMS resonant devices. First, one side of the resonant structure is backed with a vacuum-sealed cavity that not only improves the quality factor ( $Q$ ) and, thus, enhances the sensor resolution but also facilitates the process of chemical functionalization when only the top side of the structure should be coated. When the back side is not encapsulated, the chemical functionalization can unintentionally coat the back side. Second, the CMUT technology inherently features parallelism: a single CMUT resonator is composed of many resonators (or cells) electrically connected in parallel. The result is a reduced motional impedance and, thus, also a reduced thermal noise.<sup>8</sup> Moreover, the array structure enables multichannel detection to achieve improved selectivity. In addition, multichannel capability allows for

**Received:** July 20, 2011

**Accepted:** October 28, 2011

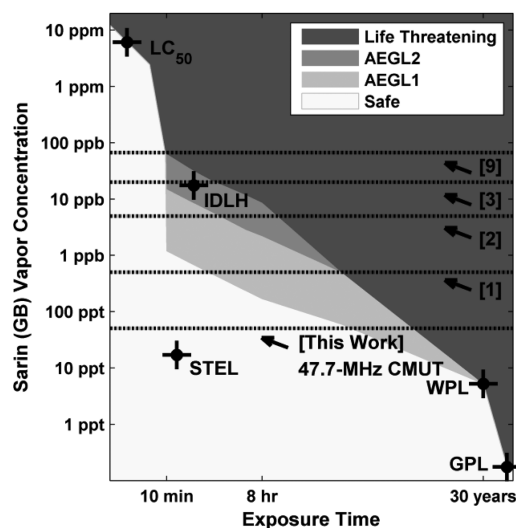


**Figure 1.** An illustration of airborne exposure limits (AELs) defined by OSHA (USA) for sarin (GB) with its respective exposure time. AELs include IDLH, STEL, worker population limit (WPL), and general population limit (GPL).<sup>11,12</sup> Lethal concentration 50 (LC<sub>50</sub>) refers to the vapor concentration that kills 50% of the test animals. Minimum detection levels ( $3\sigma$  confidence level) of highly sensitive micromachined sensors to DMMP are marked for comparison.

a reference channel to compensate for any sensor responses caused by factors other than the changes in the analyte concentration, such as ambient temperature changes.

In previous work, we developed miniaturized resonant chemical sensor systems based on CMUTs operating at 6 MHz and 18 MHz.<sup>9,10</sup> For the 18-MHz CMUT that was functionalized with polyisobutylene (PIB), we demonstrated a promising volume sensitivity of 37.38 ppb/Hz to DMMP, successful pattern recognition through principal component analysis (PCA), and a good repeatability of the sensor. However, a further improvement in volume sensitivity was required in practice for two main reasons. First, the Immediately Dangerous to Life or Health (IDLH) and Short-Term Exposure Limit (STEL) mandated levels of sarin are 17.4 ppb and 17 ppt, respectively, as determined and enforced by the Occupational Safety and Health Administration (OSHA) and the National Institute for Occupational Safety and Health (NIOSH) (Washington, D.C.);<sup>11</sup> thus, an effective portable chemical sensor for counter-terrorism application must have a sensor resolution below 17.4 ppb (Figure 1). Second, an enhanced sensitivity would allow sensors to distinguish frequency changes caused by the absorption of the analyte of interest from those caused by absorption of interference analytes. The same is valid for interferences due to changes in the environment, such as temperature and pressure.

Consequently, to meet these requirements, we have developed CMUTs optimized for chemical sensor applications.<sup>13</sup> These devices operate at a higher frequency of 47.7 MHz with an improved mass sensitivity of 48.8 zg/Hz/ $\mu\text{m}^2$ . We tested the performance of our improved sensor system using a test setup at a certified lab (MIT Lincoln Laboratory), which has the capability to deliver very low concentrations of gases in the 10 ppb to 1 ppm range. In addition, the lab setup ensures the accurate delivery of such low concentrations to the sensor system through rigorous calibration and reliable monitoring of the test environment.

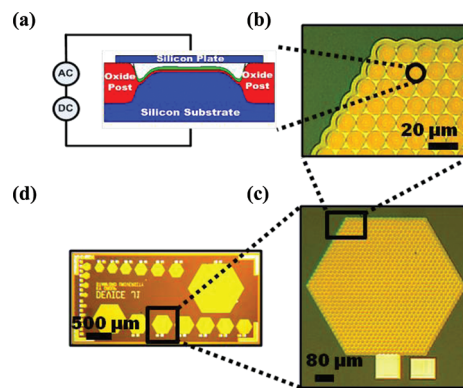


**Figure 2.** (a) Cross-section schematic of a single CMUT resonator with the biasing scheme. (b) Optical picture of a section of a CMUT resonator, illustrating that multiple resonators are connected in parallel to form an overall resonator. (c) Optical picture of a single CMUT composed of 1027 resonators placed in a hexagonal form. (d) Optical picture of a single die that consists of an array of CMUT resonators.

## ■ STRUCTURE AND OPERATIONAL PRINCIPLES OF THE CMUT SENSOR

**Sensor Structure.** The basic unit of the CMUT sensor is a circular capacitor with a highly doped single-crystal silicon plate as the top electrode and a conductive substrate as the bottom electrode. The 500-nm thick plate is suspended over a group of circularly patterned vacuum cavities with a radius of 5.3  $\mu\text{m}$  to achieve a high resonant frequency ( $f_0$ ) of 47.7 MHz, as estimated by eq 1,<sup>14</sup>

$$f_0 = \frac{0.83}{a} \sqrt{\frac{Et^3}{m(1-\nu^2)}} \quad (1)$$

where  $a$  is the radius,  $E$  is the Young's modulus,  $t$  is the thickness,  $\nu$  is the Poisson ratio, and  $m$  is the mass of the circular plate. The height of the vacuum gap is 50 nm, and the oxide posts supporting the top plate are 1- $\mu\text{m}$  thick (Figure S1 in the Supporting Information). Two aluminum contact pads provide electrical connections to the silicon plate (hot electrode) and the silicon substrate (shared ground electrode).

CMUT sensors are typically composed of hundreds to thousands of these individual circular electrostatically actuated resonators, all electrically connected in parallel (Figure 2b). The multiple-resonator configuration, composed of  $n$  resonators with uncorrelated noise, would achieve a reduction in motional impedance by a factor of  $n$  and, thus, in thermal noise by a factor of  $n^{1/2}$ .<sup>8,15</sup> The low thermal noise of a resonator in a sensor application is important because the noise determines the minimum level of detectable signal, i.e., the resolution of the system. In addition, the motional impedance of a device can be optimized by varying the number of resonators connected in parallel for good electrical impedance matching to the interface circuitry.

The 47.7-MHz CMUT presented in this paper is composed of 1027 circular resonators, packed in a hexagonal shape configuration (Figure 2c). In contrast to a rectangular or square form, the hexagonal form allows a smaller parasitic resistance on the top electrode, and it moreover reduces the ratio of the number of edge resonators to inner resonators. Minimizing this ratio is important because the edge resonators have acoustic boundary

conditions that are different from those of the inner ones, which adversely affect the total impedance of such a multiresonator.<sup>16</sup>

Twenty-two of these hexagonal CMUT sensors are fabricated in a single die to achieve an array structure (Figure 2d). The number of resonators in each device was varied in this design to experiment different device input impedance values. The array structure is essential to a sensor system that uses a mass-loading mechanism to ensure selectivity through pattern recognition. Even if a functionalization layer, such as a synthesized polymer, is specifically designed to be sensitive to the analyte of interest, the layer may still respond to other chemicals with similar chemical compositions. In addition, the resonant frequency of the CMUT sensor itself can change due to the changes in the environment, such as temperature and pressure. Thus, a multichannel detection is often employed to provide data for a pattern recognition algorithm and to provide a reference channel composed of a bare sensor to compensate for changes in the environment. The 47.7-MHz CMUT is fabricated using a high temperature assisted direct wafer-bonding in combination with local oxidation (LOCOS) technique. Details of the device fabrication have been described previously.<sup>17</sup>

**Operational Principles.** The sensing mechanism of our resonant chemical sensor is mass-loading. Equation 1 indicates that the resonant frequency of a circular plate is inversely proportional to the square-root of mass of the resonating structure. Equation 2, the derivative of eq 1, estimates that the amount of negative shift in the resonant frequency,  $\delta f_0$ , is directly proportional to the amount of loaded mass,  $\delta m$ :

$$\delta f_0 = -\frac{1}{2} \times \frac{f_0}{m} \times \delta m \quad (2)$$

By functionalizing the surface of the resonant structure with a chemically sensitive layer, the sensitivity and selectivity of this mass sensor to a targeted analyte can be significantly improved. Sorption of an analyte on the layer results in an increase in mass, which then reduces the resonant frequency by an amount proportional to the mass change.

The mass sensitivity per unit area,  $S_m$ , is a function of the geometry and material of the resonant structure, as shown in eq 3:<sup>14</sup>

$$S_m = -2 \times \frac{m}{f_0 A} = -2 \frac{\rho t}{f_0} = 4.27 a^2 \rho^{3/2} \sqrt{\frac{(1-\nu^2)}{E}} \quad (3)$$

where  $A$  represents the surface area. Thus, to achieve a high mass sensitivity, a circular plate with a smaller radius and lower density is required. Using eq 3 and the measured frequency of 47.7 MHz, we can estimate a mass sensitivity per unit area of 48.8 zg/Hz/ $\mu\text{m}^2$  for the CMUT used in this work with a radius of 5.3  $\mu\text{m}$  and a thickness of 500 nm.

## SYSTEM LEVEL DESIGN

**CMUT-Based Oscillator Design.** To track the change in resonant frequency of the sensor in real time, we designed and built a free-running oscillator using the 47.7-MHz CMUT as a frequency selective device. We first measured the sensor's electrical input impedance. An equivalent circuit model, based on the measured electrical impedance data, was used for the oscillator design.

**Electrical Characterization of the Sensor.** The electrical input impedance of the CMUT, biased at various DC bias voltages at a fixed AC amplitude of 50 mV, was measured using an impedance

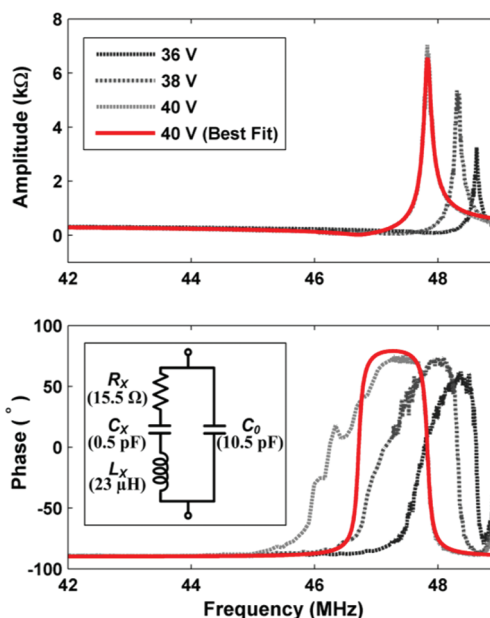


**Figure 3.** Plot of measured input impedance characteristics of the CMUT resonator biased at various DC bias voltages at a fixed AC amplitude of 50 mV, in air. The solid line represents the fitted input impedance characteristics of the CMUT resonator biased at 40 V while the inset shows the schematic of the four-element van Dyke equivalent circuit model used to fit the input impedance of the CMUT biased at a specific DC voltage. The values of the circuit components of the CMUT biased at 40 V are listed in parentheses in the inset.

analyzer (Agilent Technologies, Model 4294A, Palo Alto, CA). As expected for a capacitive resonator, the resonant frequency decreases when the DC bias voltage is increased due to spring softening effect (Figure 3).<sup>18</sup> At a higher bias voltage, the higher electrostatic force deflects the top plate closer toward the bottom electrode (in addition to the deflection due to the ambient pressure), which further increases the electrostatic force to cause additional deflection. Thus, the actual deflection is larger than that initially actuated by a given bias voltage; this effect is frequently modeled as if the spring constant of the plate is reduced. The softer spring  $k'$  is defined in

$$k' = k(1 - k_T^2) \quad (4)$$

where  $k$  and  $k'$  are the initial and final spring constants, respectively, and  $k_T^2$  is the electromechanical coupling coefficient.<sup>19</sup>

For a specific bias voltage, we fitted the input impedance to the conventional four-element Butterworth van Dyke (BvD) model (Figure 3).<sup>20</sup> The BvD equivalent circuit is composed of four circuit elements,  $R_x$ ,  $L_x$ ,  $C_x$ , and  $C_0$ , which, respectively, represent the loss, mass, inverse of stiffness, and static capacitance of the resonant structure. For example, the CMUT biased at 40 V with a series resonant frequency of 46.74 MHz and a parallel resonant frequency of 47.83 MHz can be modeled by the BvD model with values listed in Figure 3.

**Design and Characterization of the Oscillator Circuit.** We designed and built an oscillator that operates near the parallel resonance of the CMUT sensor because the quality factor at the series resonant frequency (81 at 40 V) of our device is smaller than that at the parallel resonant frequency (416 at 40 V). The cell-to-cell nonuniformity in our devices is more pronounced at the series resonance, which results in the lower quality factor

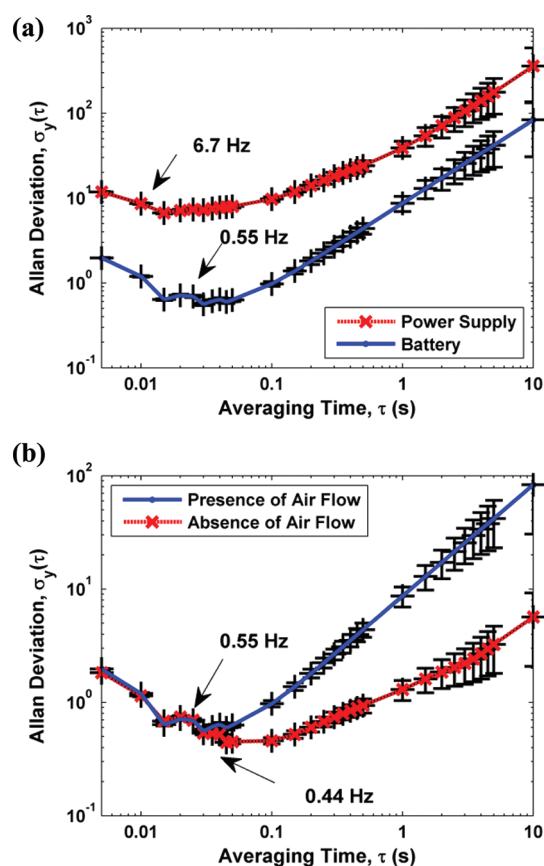


**Figure 4.** Plot of overlapped Allan deviation calculated from the frequency counter data with a gate time of 5 ms (Stanford Research Systems, Model SRS620, Sunnyvale, CA) over different averaging time. The error bars indicate the 1 $\sigma$  confidence level. Comparison of Allan deviation between (a) power supply and battery, and (b) presence (300 mL/min) and absence of carrier flow.

(Figure S2 in the Supporting Information). Specifically, to obtain a loop gain larger than one at a frequency near the parallel resonance, we placed the CMUT in the oscillator loop through a voltage divider before connecting to a voltage amplifier (Figure S3a in the Supporting Information). The signal is further amplified and band-pass filtered in a second stage, such that the loop gain and phase satisfy the Barkhausen criteria for oscillation.<sup>21</sup> In contrast to our oscillator, in a typical series-resonant MEMS resonator oscillator, the resonator would be placed in series with a trans-impedance amplifier. We implemented the parallel-resonant oscillator on a printed circuit board (PCB) with discrete components. The CMUT was directly wire-bonded to the PCB in order to minimize the parasitics (Figure S3b in the Supporting Information).

The short-term frequency stability of an oscillator is important because the noise,  $\delta f$ , determines the limit of detection (LOD) of a mass-loading-based resonant sensor, as shown in eq 2. We thus measured the short-term frequency stability in the time domain, expressing it as an overlapped Allan deviation,<sup>22</sup> using a frequency counter (Stanford Research Systems, Model SR620, Sunnyvale, CA). The overlapped Allan deviations were computed for different averaging times using the frequency data obtained at a sampling rate of 200 Hz. To investigate possible noise sources in our circuit implementation, we measured the Allan deviations of the oscillator when the circuit was powered by power supplies (Agilent Technologies, Model 6216A,

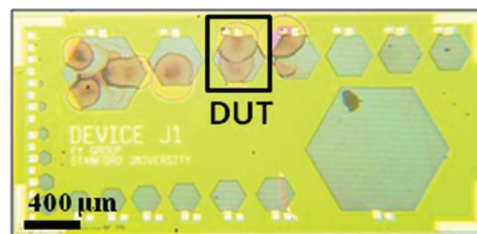


**Figure 5.** Photograph of the four CMUT resonators functionalized with an approximately 50-nm thick chemiselective layer using a pipetting method. AFM measurements in tapping mode show the edge and the center of a single droplet to be 101 and 48 nm, respectively.

Palo Alto, CA) and by  $\pm 5$  V (for amplifiers) and 40 V (for biasing the CMUT) batteries. When the oscillator was powered by batteries, the Allan deviation improved almost by a factor of 10 from  $4.2 \times 10^{-7}$  to  $3.5 \times 10^{-8}$  Hz ( $3\sigma$ ) (Figure 4a). In addition, to estimate a practical noise floor of the system that includes the effects of fluctuations in the gas flow due to the mass flow controllers, we measured the frequency noise both in the presence and the absence of the gas flow. The lowest Allan deviation of  $2.77 \times 10^{-8}$  ( $3\sigma$ ) and  $3.5 \times 10^{-8}$  ( $3\sigma$ ) and the corresponding frequency noise of 1.32 Hz ( $3\sigma$ ) and 1.65 Hz ( $3\sigma$ ) were estimated at an averaging time of 30 ms, respectively, in the absence and the presence of the gas flow at 300 mL/min (Figure 4b). Using eq 2 and the frequency noise measured in the presence of the gas flow, we estimated the mass resolution value to be  $80.5 \text{ zg}/\mu\text{m}^2$  (i.e.,  $80.5 \times 10^{-21} \text{ g}/\mu\text{m}^2$ ).

**Functionalization.** The CMUT mass sensor was converted to a chemical sensor that is targeted to detect DMMP through functionalization. An approximately 50-nm thick layer of DKAP polymer, which was developed at Sandia National Laboratory (Livermore, CA) to be highly sensitive to DMMP, was pipet-dropped on top of four sensors (Figure 5). Because the polymer was delivered using a hand-held pipetting device, the reproducibility of the layer deposition was not great in terms of area coverage and thickness. To obtain a more uniform layer, other methods such as inkjet printing should be used. DKAP polymer is a poly(dimethylsiloxane) derivative with a glass transition temperature  $T_g$  of  $\sim 20$  °C.<sup>23</sup> The functionalization layer must be thick enough to absorb the analyte and at the same time thin enough not to significantly load the resonant sensor. By comparing the impedance of the device before and after the coating (not shown), we determined that the approximately 50-nm thick coating on the 500-nm CMUT resonant plate only resulted in a 0.65% change in the parallel resonant frequency. However, the quality factor at parallel resonance was degraded by almost 55% due to the damping from the polymer film and due to the increase in cell-to-cell variations from nonuniformities in the polymer film coating.

**Experimental Chemical Setup.** We evaluated the performance of the 47.7-MHz sensor system in the ppb range of DMMP concentrations at an outside laboratory (the MIT Lincoln Laboratory). Through the Micro Gas Analyzers (MGA) program sponsored by the Defense Advanced Research Projects Agency (DARPA), the MIT Lincoln Laboratory has established a chemical setup that not only delivers vapor concentration as low as 10 ppb but also ensures precise and accurate delivery through stringent calibration. Due to the limited number and types of equipment available,<sup>9,10</sup> the lowest vapor concentration of DMMP that our in-house chemical setup can reliably deliver is 3.2 ppm. Using the MIT Lincoln Laboratory setup, we conducted a preliminary

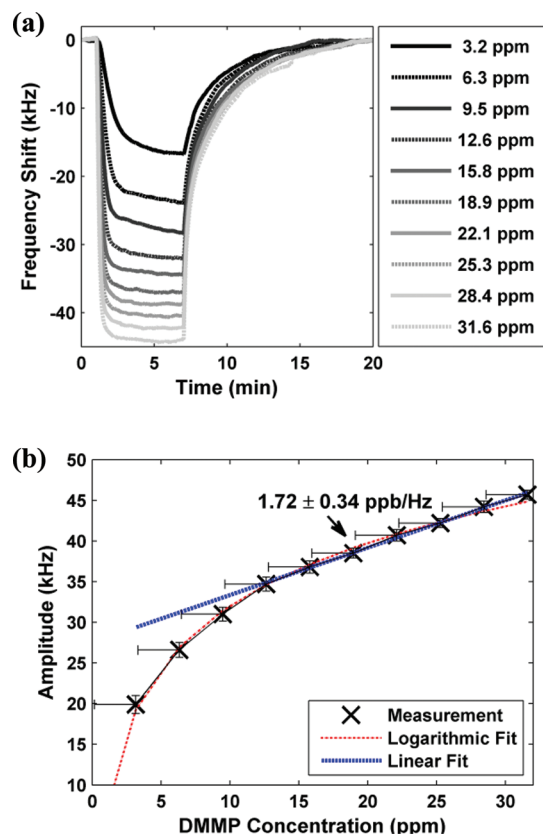


**Figure 6.** (a) Transient frequency shifts in response to various concentrations of DMMP in  $N_2$  that were delivered using the in-house chemical setup. DMMP vapor starts to flow in at 60 s and stops at 420 s. (b) Plot of maximum frequency shift observed at different DMMP concentrations with the error bars indicating  $3\sigma$  confidence on the frequency shifts measured over 3 days.

sensitivity test of the improved sensor with a higher mass sensitivity and a more sensitive polymer layer. The preliminary volume sensitivity of our sensor to DMMP in  $N_2$  was  $1.72 \pm 0.34$  ppb/Hz (Figure 6), which attested to a need for an advanced setup that would deliver lower vapor concentrations in the ppb range. Furthermore, assuming the close similarity of DMMP and sarin gas, the recommended IDLH level for airborne exposure to sarin is 17 ppb, which required us to experimentally demonstrate our sensor response to at least 10 ppb of DMMP vapor concentration.

Any chemical setup that is claimed to deliver a ppb-range of vapor concentration must be calibrated because the systematic errors and offsets in the vapor-delivery system are no longer negligible and must be accounted for. For example, a setup based on the saturation bubbler method has a systematic error of overestimating vapor concentrations and thus underestimating the sensor performance.<sup>24</sup> The saturation bubbler method computes the concentration based on the assumption that the bubbler generates a fully saturated gas phase through the enlarged gas–liquid contact area from the bubbles. However, in practice, the gas enclosed in the bubbles could be partially saturated, for example, due to short travel-time of bubbles in the liquid. In addition, other factors, such as liquid level in the bubbler and temperature dependency of vapor pressure of the liquid, attributes to the uncertainties in the generated vapor concentrations. To ensure delivery of accurate concentration below 1 ppm, we tested our sensor at the MIT Lincoln Laboratory where delivery

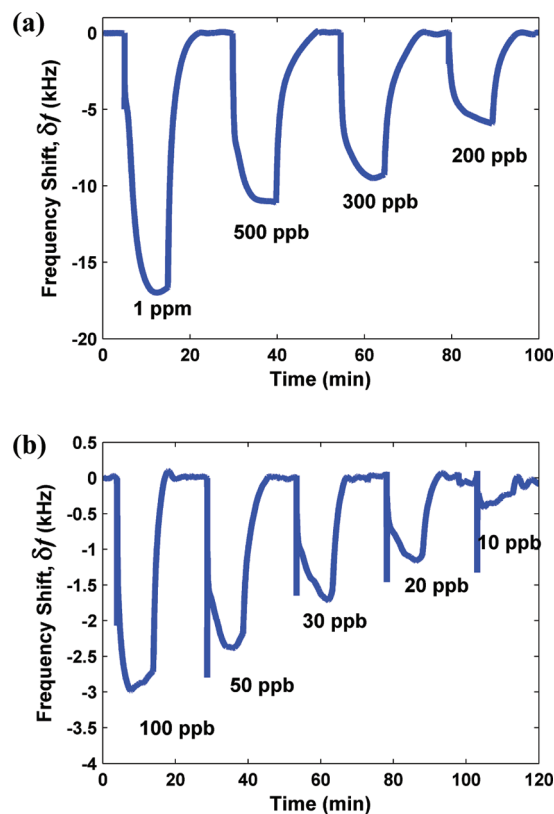


**Figure 7.** Transient frequency shifts in response to (a) concentrations from 1 ppm to 200 ppb and (b) concentrations from 100 to 10 ppb of DMMP. DMMP vapor starts to flow in at 5 min and stops at 15 min followed by 10-min purging with the carrier gas.

of various concentrations was calibrated through high-performance gas analyzers including a gas chromatograph mass-selective detector (Agilent 6890/5973N).

The chemical setup at the MIT Lincoln Laboratory is designed to deliver a concentration of an analyte as low as 10 ppb over three decades of concentrations (Figure S4 in the Supporting Information). The sources of analyte gases, both placed in a constant-temperature oven, are permeation tubes for low concentrations (1 ppb to 1 ppm) and bubblers for high concentrations (1 ppm to 10 ppm). The various vapor concentrations are then generated by using mass flow controllers to adjust the ratio of the analyte concentration to the carrier gas concentration. When the concentration is generated through two mixing stages, the quantification limit of their setup is 1 ppb. The carrier gas used for our test was air that was first dehydrated and then purified through a zero-air generator (Model 76-803, Balston Parker, Haverhill, MA). The mixed gas containing the purified air and DMMP was then delivered to a small chamber ( $0.8 \text{ cm}^3$ ) that enclosed the functionalized CMUT device (Figure S5 in the Supporting Information).

## EXPERIMENTAL RESULTS AND DISCUSSION

We measured the transient frequency shifts in response to nine different analyte concentrations of DMMP ranging from 1 ppm down to 10 ppb (Figure 7). As predicted, the oscillator frequency decreased when the polymer absorbed the DMMP molecules by an amount proportional to the DMMP concentration. The frequency then returned to the baseline when the chamber was purged with the carrier gas and the polymer

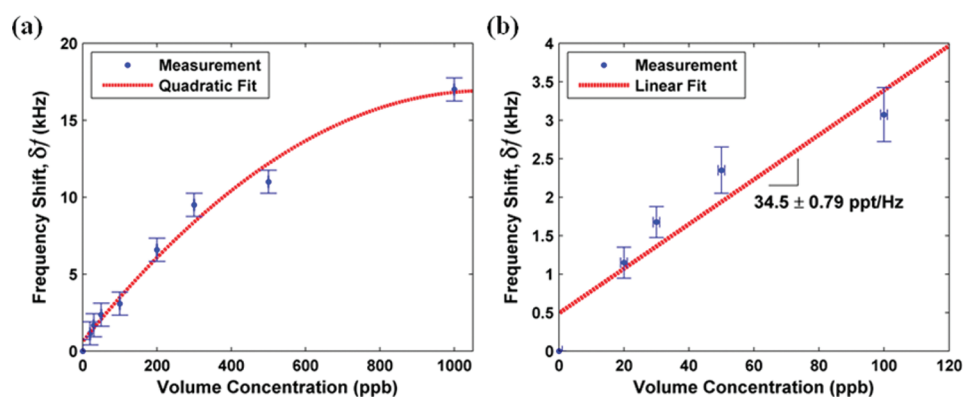


**Figure 8.** (a) Plot of maximum frequency shift observed at different DMMP concentrations with error bars, and (b) zoom-in plot toward the low concentrations showing a linear-fit.

released the DMMP molecules. For relatively low concentrations ranging from 10 to 100 ppb, the observed maximum frequency shifts are linearly proportional to the vapor concentrations (Figure 8b). As the DMMP concentration increased above 100 ppb, the maximum frequency shifts continued to increase but at smaller increments, possibly because the 50-nm thick polymer layer began to saturate (Figure 8a).

In the linear regime of 10 and 100 ppb, we used the best-fit linear regression to estimate the slope and compute a volume sensitivity of  $34.5 \pm 0.79$  ppt/Hz by taking the inverse of the slope. Not only is this volume sensitivity higher by orders of magnitude compared to that of our previous sensor system,<sup>10</sup> but it is also, to the authors' knowledge, the highest volume sensitivity demonstrated so far for a resonant sensor system without any surface modification such as surface roughening or porous surface to enhance the sensitivity (Table S1 in the Supporting Information). In addition, based on the system noise floor of 1.65 Hz ( $3\sigma$ ), we achieved an unprecedented limit of detection of 50.5 pptv.

Sharp spikes on the order of  $\sim 3$  kHz shift, which were prominent at low concentrations up to 50 ppb due to the comparable frequency shifts caused by the absorbance of DMMP, were observed at the beginning of each DMMP pulse (Figure 7). These sharp spikes were caused by the sudden pressure change in the system when the mass flow controller connected to the DMMP permeation tubes was opened. Because the CMUT is a flexural mode resonator with a top plate exposed to the medium, a pressure change in the medium results in a change in the deflection and thus in the resonant frequency.

The response time to the pressure change in comparison to that to the mass change is much smaller, which allows the system to distinguish between the two events. By fitting the curve with an exponential function, we computed the average fall time constants,  $t_{90}$ , to 90% of full response to both a pressure change and a mass change. The fall  $t_{90}$  were 0.71 and 117 s to the pressure and the mass change, respectively. In addition, the response time to mass change is reasonable for a real-time application and is comparable to that of the other sensor systems (Table S1).

To evaluate the selectivity of the polymer to DMMP, we measured the transient frequency response of our sensor to three different concentrations of two other analytes, dodecane and 1-octanol. At 1 ppm and 100 ppb concentrations, the frequency shifts in response to dodecane and 1-octanol are much smaller than to DMMP (Table 1). At the low concentration of 10 ppb,

**Table 1. Summary of Maximum Frequency Shifts in Response to Dodecane, 1-Octanol, and DMMP at Various Concentrations**

concentration	10 ppb	100 ppb	1 ppm
DMMP	637	2949	16650
dodecane	152	652	2830
1-octanol	365	1620	2301

the frequency shift in response to DMMP is still the largest, but the distinction between the three analytes is smaller. This result validates that this polymer is selective to DMMP in comparison to other volatile compounds. However, to achieve the selectivity of the resonant sensor to differentiate different chemicals, we would need to implement multichannel detection with pattern recognition, which is part of our future work.

## CONCLUSION

This paper has presented a CMUT-based chemical sensor system that is a strong candidate for use in future chemical sensor systems because of features that include a high quality factor and massive parallelism resulting from its inherent uniform array structure. This system uses a 47.7-MHz CMUT resonant sensor with a mass resolution per plate area of  $0.048 \text{ ag}/\mu\text{m}^2$  as the physical mass sensor, which was functionalized with the DKAP polymer developed at the Sandia National Laboratory. The high sensitivity of 34.5 ppt/Hz was measured at the MIT Lincoln Laboratory, where a calibrated, reliable, and accurate chemical setup for the ppb-range chemical delivery was provided. Using the low noise floor of the oscillator, we also achieved a high resolution of 51 pptv ( $3\sigma$ ). Assuming there is a close similarity between DMMP and sarin gas, the presented sensor is not only sufficient to detect IDLH of sarin gas but also has the highest potential among those reported to detect sarin gas close to the STEL level.

## ASSOCIATED CONTENT

**S Supporting Information.** Additional information as noted in text. This material is available free of charge via the Internet at <http://pubs.acs.org>.

## AUTHOR INFORMATION

## Corresponding Author

\*E-mail: hyunjoo@stanford.edu.

## ACKNOWLEDGMENT

We thank Defense Advanced Research Projects Agency, Microsystems Technology Office, for their financial support of this project through grant N66001-06-1-2030. We also thank Joe Simonson at Sandia National Laboratory for drop-coating the polymer on our device and Mike Switkes at the MIT Lincoln Laboratory for the advanced chemical setup.

## REFERENCES

- (1) Snow, E. S.; Perkins, F. K.; Houser, E. J.; Badescu, S. C.; Reinecke, T. L. *Science* **2005**, *307*, 1942.
- (2) Robinson, J. T.; Perkins, F. K.; Snow, E. S.; Wei, Z. Q.; Sheehan, P. E. *Nano Lett.* **2008**, *8* (10), 3137–3140.
- (3) Voiculescu, I.; Zaghoul, M. E.; McGill, R. A.; Houser, E. J.; Fedder, G. K. *IEEE Sens. J.* **2005**, *5* (4), 641–647.
- (4) Kirianaki, N. V.; Yurish, S. Y.; Shpak, N. O.; Deynega, V. P. *Data acquisition and signal processing for smart sensors*, 1st ed.; Wiley: New York, 2002.
- (5) Battiston, F. M.; Ramseyer, J.-P.; Lang, H. P.; Baller, M. K.; Gerber, Ch.; Gimzewski, J. K.; Meyer, E.; Guntherodt, H.-J. *Sens. Actuators, B* **2001**, *77* (1–2), 122–131.
- (6) Zhang, H.; Kim, E. S. *J. Microelectromech. Syst.* **2005**, *14* (4), 699–706.
- (7) Wohltjen, H.; Snow, A. W.; Barger, W. R.; Ballantine, D. S. *IEEE Trans. Ultrason., Ferroelec., Freq. Control* **1987**, *34*, 172–178.
- (8) Vig, J. R.; Kim, Y. *IEEE Trans. Ultrason., Ferroelec., Freq. Control* **2002**, *46* (6), 1558–1565.
- (9) Park, K. K.; Lee, H. J.; Yaralioglu, G. G.; Oralkan, Ö.; Kupnik, M.; Quate, C. F.; Khuri-Yakub, B. T.; Braun, T.; Lang, H. P.; Hegner, M.; Gerber, C.; Gimzewski, J. *Appl. Phys. Lett.* **2007**, *91*, 094102.
- (10) Park, K. K.; Lee, H. J.; Kupnik, M.; Oralkan, Ö.; Khuri-Yakub, B. T. *Sens. Actuators, B* **2011**, *160* (1), 1120–1127.
- (11) National Institute for Occupational Safety and Health. The Emergency Response Safety and Health Database. [http://www.cdc.gov/NIOSH/ershdb/EmergencyResponseCard\\_29750001.html](http://www.cdc.gov/NIOSH/ershdb/EmergencyResponseCard_29750001.html) (accessed Oct 17, 2011)
- (12) U.S. Army Public Health Command. Chemical Agent Health-Based Standards and Guidelines Summary. <https://phc.amedd.army.mil/> (accessed Oct 17, 2011)
- (13) Lee, H. J.; Park, K. K.; Kupnik, M.; Oralkan, O.; Khuri-Yakub, B. T. Presented at IEEE Sensors 2010, IEEE International Conference on Sensors, Waikoloa, Hawaii, Nov 1–4, 2010.
- (14) Meirovitch, L. *Analytical Methods in Vibrations*, 1st ed.; Macmillan: New York, 1967.
- (15) Lee, H. J.; Park, K. K.; Cristman, P.; Oralkan, Ö.; Kupnik, M.; Khuri-Yakub, B. T. Presented at 22nd IEEE International Conference on Micro Electro Mechanical Systems, Sorrento, Italy, Jan 25–29, 2009.
- (16) Park, K. K.; Kupnik, M.; Lee, H. J.; Wygant, I. O.; Khuri-Yakub, B. T. Presented at the IEEE Ultrasonics Symposium, San Diego, CA, Oct. 11–14, 2010.
- (17) Park, K. K.; Lee, H. J.; Kupnik, M.; Khuri-Yakub, B. T. *J. Microelectromech. Syst.* **2011**, *20* (2), 95–103.
- (18) Mason, W. P. *Electromechanical Transducers and Vme Filters*; D. Van Nostrand Company Inc.: London, 1948.
- (19) Fraser, J. D.; Reynolds, P. J. *Acoust. Soc. Am.* **2000**, *108* (5), 2599–2599.
- (20) Sherrit, S.; Wiederick, H. D.; Mukherjee, B. K. *Proc. - IEEE Ultrason. Symp.* **1997**, *2*, 931–935.
- (21) Singh, V. *Analog Integr. Circuits Signal Process.* **2010**, *62*, 327–332.
- (22) Allan, D. *IEEE Trans. Ultrason., Ferroelec., Freq. Control* **1987**, *34* (6), 647–654.

(23) Li, M.; Myers, E. B.; Tang, H. X.; Aldridge, S. J.; McCaig, H. C.; Whiting, J. H.; Simonson, R. J.; Lewis, N. S.; Roukes, M. L. *Nano Lett.* **2010**, *10* (10), 3899–3903.

(24) Barratt, R. S. *Analyst* **1981**, *706*, 817–849.